Techno-economic assessment of a Multi-effect Distillation plant installed for the production of irrigation water in Arica (Chile)

Palenzuela, P.[(1)*], Miralles-Cuevas, S.[(2,3)], Cabrera-Reina, A.[(2, 3)], Cornejo-Ponce, L. [(2, 3)**]

[(1)] CIEMAT-Plataforma Solar de Almería, Ctra. de Senés s/n, 04200 Tabernas, Almería, Spain

[(2)] Laboratorio de Investigaciones Medioambientales de Zonas Áridas (LIMZA), Universidad de Tarapacá. Av. General Velásquez 1775, Arica, Chile

[(3)] Escuela Universitaria de Ingeniería Mecánica (EUDIM), Universidad de Tarapacá. Av. General Velásquez 1775, Arica, Chile

Corresponding author 1: Ph.D. Patricia Palenzuela Ardila, (Plataforma Solar de Almería), patricia.palenzuela@psa.es

Corresponding author 2: Ph.D. Lorena Cornejo Ponce (Universidad de Tarapacá), lorenacp@uta.cl

Abstract

In the context of a regional Chilean project (FIC Taltape project, BIP code 30158422-0), a multi-effect distillation (MED) pilot plant has been built and installed in a small community in the north of Chile (Taltape, Arica) in order to supply treated water for agricultural and domestic purposes. The aim of this paper is to assess the techno-economic feasibility of this system for supplying water with the required quality to the population. The characterization of the feed water and the effluents from the MED pilot plant (distillate and brine), obtained during five months of operation, has been firstly performed. Then, the prediction of the operation of the water treatment system with solar energy has been carried out using a typical meteorological year and the design of a static solar field that cover the thermal energy needs of the water treatment plant.

The annual simulations of the MED pilot plant operating with solar energy showed that the water needs can be mostly covered using a static solar thermal field with a total area of

113.2 m^2, which would generate roughly 46% of the total heat required by the water treatment plant. The technical analysis has been completed with an exhaustive economic assessment. The specific water costs have been determined for the MED pilot plant and the scale factor when the productivity is increased up to 5,000 m^3 / day has been evaluated. The cost of distillated water produced by the MED plant varied from 15.0 USD$/m^3 for the 10 m^3/day production capacity to 1.25 USD$/m^3 when this variable is increased to 5,000 m^3/day.

Keywords: Multi-effect distillation, brackish water treatment, arsenic and boron removal, modelling and simulation, solar thermal water treatment

Nomenclature

R	Retention percentage (%)
C_{BFW}	Concentration of the element in the brackish feed water (mg/L)
C_D	Concentration of the element in the distillate (mg/L)
$\Delta T_{eff,i}$	Temperature difference between effects (ºC)
T_v	Vapour temperature inside the effect (ºC)
N	Number of effects
Q_s	Heat transfer rate provided to the first effect (kW)
T_s	Temperature of the heating energy source supplied to the first effect
M_s	Steam mass flow rate supplied as the heating energy source to the first effect (kg/s)
λ_s	Change in enthalpy related to the condensation of the steam supplied to the first effect (kJ/kg)
U_e	Overall heat transfer coefficient (kW/m^2·ºC)
M_f	Feedwater mass flow rate (kg/s)

M_{gb}	Total vapour generated inside the effect (kg/s)
λ_{gb}	Latent heat of vaporization (kJ/kg)
C_p	Specific heat (kJ/kg·ºC)
T_f	Temperature of the feedwater that reaches the first effect (ºC)
M_{prod}	Total distillate obtained from the water treatment plant (kg/s)
RR	Recovery Ratio
sA	Specific area (kg/m^3/day)
STC	Specific thermal consumption (kWh/m^3)
GOR	Gain Output Ratio
θ	Incidence angle (º)
η_{opt}	Optical efficiency (%)
G_k	Global irradiation over tilted plane (W/m^2)
T_{amb}	Ambient temperature (ºC)
$\dot{m}$	Mass flow rate through the solar collector (kg/s)
T_{col}	Average between the inlet and outlet temperatures of the collector (ºC)
T_{in}	Inlet water temperature in the solar collector (ºC)
T_{out}	Outlet water temperature in the solar collector (ºC)
$K_{\tau\alpha}$	Incident angle modifier
A_a	Aperture area of the collector (m^2)
C_B	Approximate cost of equipment (USD$)
C_A	Known cost of equipment (USD$)
S_B/S_A	Ratio known as the size factor
n	Size factor’s exponent

$SCOW$	Simplified Cost of Water ($USD/m^3)
M_W	Annual volume of water produced (m^3)
C_F	Annual fixed costs ($USD)
C_v	Operating cost ($USD)
I_o	Initial capital investment ($USD)
α	Amortization factor
i	Discount rate
t	Depreciation period (year)
$C_{consumables}$	Consumables costs ($USD)
C_{staff}	Staff costs ($USD)
$C_{maintenance}$	Maintenance costs ($USD)
P_e	Total electric power consumed by the MED plant (kW)
N_{col_series}	Number of collectors in series in a row
N_{rows}	Number of rows
N_{total}	Total number of collectors
A_T	Total aperture area (m^2)

1. Introduction

Water is a vital resource for both human and economic development, so it is not surprising that the absence or scarcity of water resources is directly related to poverty. Humanity faces a water scarcity problem that grows in a sustained and almost exponential way. According to the World Health Organization (WHO), 844 million people do not have easy access to an improved source of drinking water; furthermore, this number exceeds two billion people if this includes the access to enough water volume (WHO and UNICEF, 2017). This problem is related to governments and institutions around the world, so there are national policies in many countries which aim to achieve universal access to safe water. Two-thirds of the 94 countries of the United Nations recognize drinking water and hygiene services as a universal human right and 80% of them have approved national policies in this regard. However, only a quarter of them are carried out as they were established. Despite the remarkable efforts being made worldwide in the field of water, the United Nations institution highlights the fundamental need to increase investment, build human capital and obtain reliable data on which to base global actions (GLAAS Report, 2014).

Atacama Desert, which is considered the most arid one in the world, has annually less than 10 mm of precipitation per year, presenting isolated areas that only have water coming from rivers and groundwater. Nevertheless, these waters have in many cases a high content of salts, arsenic and boron and, therefore, they are neither suitable for human consumption nor for agricultural and aviculture purposes. This fact limits the development of many locations in the region which only economic resources are selling agricultural products (Bundschuh et al., 2012).

The presence of arsenic and heavy metals in the environment is a very acute problem in Latin America (Bundschuh et al., 2010). Arsenic is highly toxic in its inorganic form and its presence is mainly associated with altiplanic quaternary volcanism in the north of Chile. According to the WHO-2016 (WHO, 2016) over 226 million people worldwide are estimated to be drinking contaminated water, with an arsenic contaminant level above the 10 µg/L that WHO establishes as a maximum. This situation can lead to chronic arsenic poisoning (arsenicosis) of which skin lesions and skin cancer are the most characteristic effects (Bhattacharjeea, 2013; Hong-Jie et al., 2014; López et al., 2012; Yunus et al., 2011). According to the FONDECYT REGULAR 2011 project results, (FONDECYT REGULAR

2011, “An evaluation of the distribution, mobility and bioavailability of the arsenic present in soil and water in the Valley of Camarones, Chile: study of the levels of transference and the accumulation of arsenical species in native plants and crops” Code: 1120881) where an evaluation of the distribution and mobility of the arsenic present in soil and water was performed, the water in the Arica and Parinacota Region presents different levels of arsenic, both As(III) and As(V) species. The highest levels, more than 100 times higher than the levels established by national and international institutions (Decreto Supremo 143/2009; Decreto Supremo 144/2019; Directive 98/83/EC) are found in the Valley of Camarones. This problem presents a difficult solution, as the arsenic cannot be easily destroyed and can only be converted into different forms or transformed into insoluble compounds in combination with other elements, such as iron (Choong et al., 2007).

One of the most affected areas in the valley of Camarones is the Taltape community, where the inhabitants economy is mainly based on the exploitation of small agricultural estates, with low-valuable products such as alfalfa, and the production of meat, milk and cheese (mainly from cattle and goats). Due to the above mentioned situation, the generated products contain As and, consequently, these cannot be introduced in the legal markets, which affects the local development. For this reason, there is an important need to solve the water quality problem in a sustainable way so that this location can be established as an agricultural oasis in the middle of the desert, which would allow growing higher added value products such as tomato and/or onion, among others.

One of the possible solutions to face up this problem is desalination. Reverse osmosis (RO), multi-stage flash (MSF) and multi-effect distillation (MED) account for more than 94% of the worldwide desalination capacity (Li, 2013). The only desalination technology implemented in the Arica and Parinacota Region so far has been RO. However, in spite of its excellent salt rejection characteristics, it presents very low boron and As (III) removal efficiencies (Abejón et al., 2015; Bick et al., 2005; Hilal et al., 2011; Kang et al., 2000; Ning, 2002; Öztürk et al., 2008; Wang et al., 2016). Apart from that, further problems such as red algae blooms make RO desalination more disadvantageous versus the thermal desalination technologies, which are more robust under these particular conditions. The thermal processes also have some other advantages with respect to membrane processes, like: easier operation and maintenance that make their installation possible in countries with lack of experienced personnel, higher purity of the produced distillate and capability to deal with harsh high temperature and salinity feed waters or even with contamination (Palenzuela et al., 2014). Among thermal desalination plants, MED technology is the preferred choice due to its low top brine temperature, typically less than 70 ºC, and its low specific energy consumption requirements (Yang and Lior, 2006). On the other hand, the usual coincidence in many locations of fresh water shortage and high isolation levels make the combination of MED processes with solar energy a perfect combination to tackle the water scarcity problem in a sustainable way. Some countries of MENA region (as Qatar, Morocco, etc) and South America (mainly Chile) are more and more promoting the use of solar energy to meet its growing energy and fresh water demands (Darwish et al., 2013; Mohtar and Darwish, 2013; Hanel and Escobar, 2013; Valenzuela et al., 2017).

In the context of a regional Chilean project (FIC Taltape project, BIP code 30158422-0), a MED plant to treat brackish water containing As and Boron was installed in the Taltape community. The plant has a fresh water production capacity of 10 m^3/day and is driven by thermal energy from a biomass boiler. The electricity required is taken both from a photovoltaic solar field and from a diesel generator (backup). The feasibility of the MED process has been tested with large-scale fossil plants for many years, especially in the Gulf countries. However, there are not many solar MED units in operation. One of the solar MED plants with more operation hours is located at the Plataforma Solar de Almería (PSA). This MED unit presents a freshwater production capacity of 72 m^3/day and it is coupled to a static solar field. Several research works have been published in the scientific literature, which analyse the distillate production and the thermal efficiency of this plant at different operating conditions (Fernández-Izquierdo et al., 2012; Palenzuela et al., 2016; Chorak et al., 2017). The best operating conditions to maximize the distillate production found for this plant was to work at the maximum outlet temperature from the solar field and maximum value of the feed water flow rate in summer months and at minimum vapour temperature in the condenser and maximum outlet temperature from the solar field in winter months (Chorak et al., 2017). There is another solar MED plant located in Abu Dhabi, which is one of the first plants to be installed (120 m^3/day capacity) (El-Nashar and Ishii, 1985), although not much data have been reported from its operation. Only one test campaign developed in this solar MED plant has been published in the literature and it was focused on the validation of a steady-state model (El-Nashar and Qamhiyeh, 1995). The results showed that the product water flow rate increased from 4 to 7 m^3/h with the increase in the heating water temperature and it remained almost constant with the change in the heating water flow rate. On the other hand, it was observed that the specific heat consumption increased from 40 to 50 kcal/kg distillate when the heating water temperature rose from 65 to 75 ºC. As far as the authors' knowledge, there are no techno-economic studies in the scientific literature that address the use of MED plants with solar energy to obtain treated water for agricultural purposes.

The goal of this study case is to carry out a techno-economic assessment of a MED plant with eight effects to treat brackish water from Camarones River located in Taltape (Arica and Parinacota Region, Chile), which presents high As and Boron content, for agricultural and domestic purposes. For the technical analysis, an initial characterization of the feed water and the effluents from the MED plant (distillate and brine) obtained during several months of operation, has been performed. Then, a design model of the MED plant has been developed and implemented in Matlab with simulation purposes. The plant is currently coupled to a biomass boiler that provides the thermal energy required to operate the MED plant and to a photovoltaic solar field and a diesel generator (as back-up) for the electricity requirements of the distillation plant. The biomass boiler will be replaced by a thermal static solar field that is sized in the present work as the main element to provide the thermal energy to the MED plant, using the boiler as a backup when the solar energy is not available. Moreover, the thermal static solar field has been designed and a model of this field that predicts the hourly thermal power provided to the MED unit along the year has been developed using a typical meteorological year. This model also determines the annual solar fraction, which is the relation between the amount of energy obtained through the used solar technology and the total annual energy required by the process. Finally, the annual freshwater production has been determined and an economic analysis has been performed including the plant scale in order to provide different amounts of fresh water up to 5,000 m^3 / day.

2. Description of the system installed

2.1. Multi-Effect Distillation plant

The MED pilot plant of Taltape (see the flow diagram in Fig. 1), manufactured and delivered by INERCO Tratamiento de Aguas S.A. (Madrid, Spain) in 2016 consists of simultaneous evaporation processes of brackish water and subsequent vapour condensation at decreasing pressures and temperatures from the first effect to the last one. This plant has eight effects and each one consists in a submerged tube heat exchanger provided by AURUM Processes Company (Murcia, Spain), through which steam flows as thermal energy source. The brackish water comes from the Camarones River and is firstly collected in a reserve tank (RT1, 10 m^3) and pre-treated by microfiltration (25μm cartridge filter) before starting the distillation process. From RT1, water is pumped to the MED plant (24.3 m^3/h). Among the total flow rate, 23 m^3/h are pumped to the end condenser for refrigeration and 0.8 m^3/h of feed water (pre-treated in a sand filter) is sent to the first effect of the MED plant after flowing through the preheaters. The remaining flow rate (0.5 m^3/h) is used to cool down the vacuum pump (VP1) working on the brackish water circuit (see Fig. 1). Another vacuum pump (VP2) is cooled by the distillate water circuit. These two vacuum pumps are used to discharge the brine and the distillate outside the plant, also providing the necessary vacuum conditions in the process.

The first effect is heated with hot water coming from a biomass boiler (20 m^3/h, 70°C). The brackish water enters the first effect passing through all the pre-heaters and part of it is evaporated generating steam that is later used as the thermal energy source for the following effect. The brackish water that has not been evaporated in the first effect (called brine), goes to the second effect where there is partially evaporated by the steam entering the second effect that transfers its latent heat to the brine. The steam is then condensed, being the first distillate of the process. In order to maximize the energetic efficiency of the plant, this condensate enters the next effect along with the steam that has been already produced in the previous effect. The same process is repeated for the rest of effects.

The extraction of the distillate and brine is obtained by means of two vacuum pumps (VP 1 and 2), one for each circuit. In order to facilitate the extraction of both streams, two small reservoir deposits (0.2 m^3) were installed, one for each stream. When these reservoirs accumulate enough volume, the distillate/concentrate is extracted by the corresponding pump to another reservoir tank (RT 2, 5 m^3). Later, in a third reservoir tank (RT3, 10 m^3) the produced distillate water is post-treated to achieve irrigation and domestic water characteristics (post-treatment). Finally, the brine is mixed with the outlet of the cooling stream and returned to the Camarones River (see Fig. 1). Notice that the brine represents only 1- 2% of the total waste volume, so the mixture that finally is spilt into the river does not damage the ecosystem.

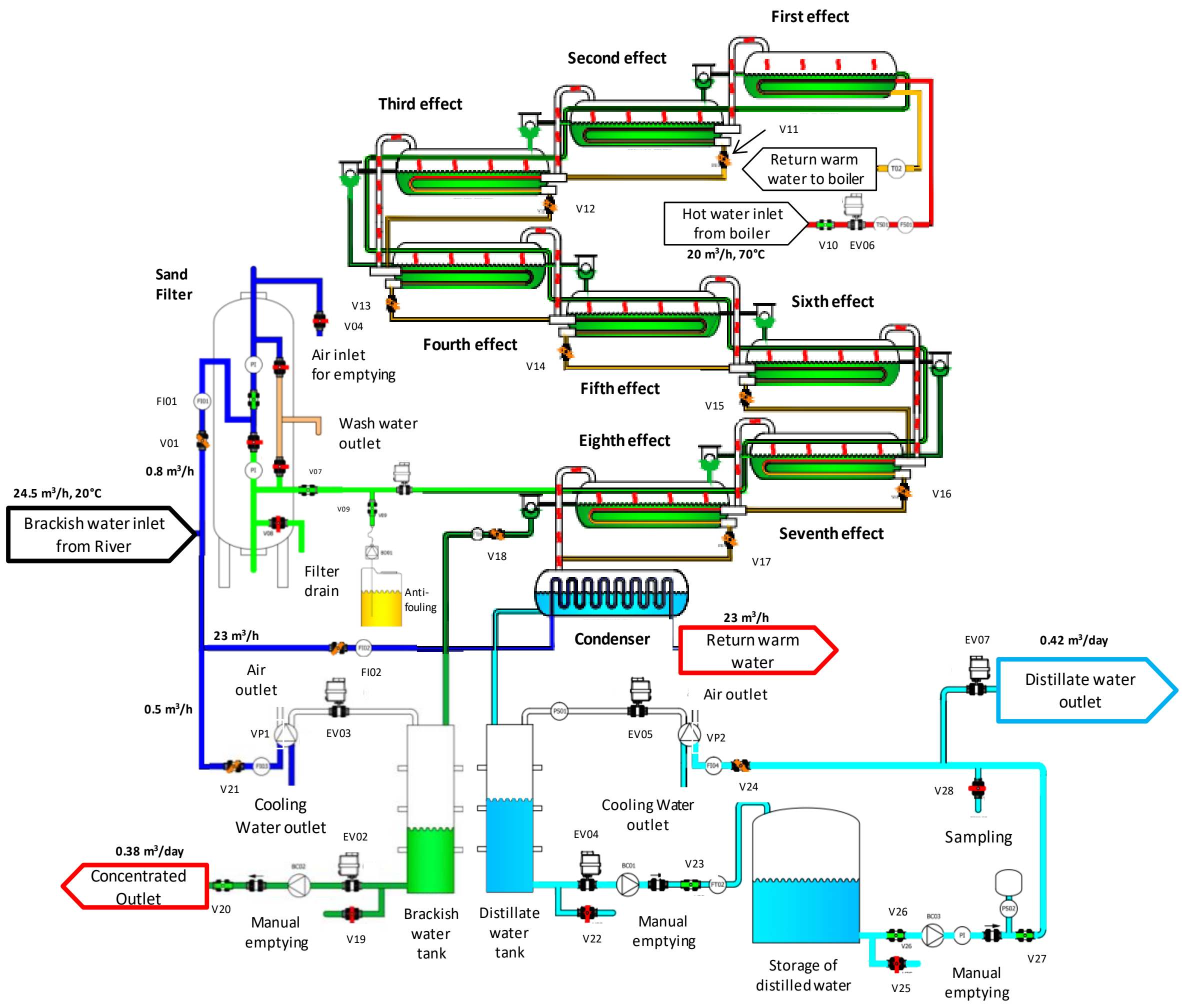

Fig. 1. Scheme of MED system

2.2 Energy supply systems

The energy supply, electricity and thermal energy, for the MED plant is done by a photovoltaic (PV) solar field and a diesel generator for the electricity requirements and by a biomass boiler for the thermal energy requirements. Fig. 2 shows a scheme of how the installed MED unit is coupled to the mentioned energy supply systems. The PV solar field consists in 10 PV panels of polycrystalline silicon. The panels are tilted 19º (local latitude). The dimensions of each panel are 1,640x990x40 mm with 60 cells per panel. The total surface is 15.8 m^2 with 3.1 kW_p (P_{max} per panel = 320W). Four stationary batteries of Lithium 12V 250 AH are available in the system. The Diesel generator was provided by VIELCO Company, KIPOR PRO-X model KDS28SS3. It has an output of 21.3 kVA (17 kW) and works at 1500 rpm with cosΦ= 0.8, at 230 or 400 V. The necessary electricity for the whole system (MED production of 10 m^3/day) is considered as 12 kW corresponding to: (i) MED plant (5 kW), (ii) 4 pumps outside (3 x 2 kW and 1 x 0.5 kW) and (iii) the boiler (0.5 kW). The electricity is provided only by the PV system during the sun hours and diesel generator is used as backup during the night.

The biomass boiler was provided by Nueva Energía, Biocalora serie 2000 model B-MAX 50. It has a rated thermal input of 50 kW and the heating surface is between 600 – 900 m^2, being fuel type pellets DIN Ø 6 mm ÷ L = 5 – 30 mm. The boiler performance is 90.1% with 2 bars of pressure max and 90 °C of maximum operation temperature.

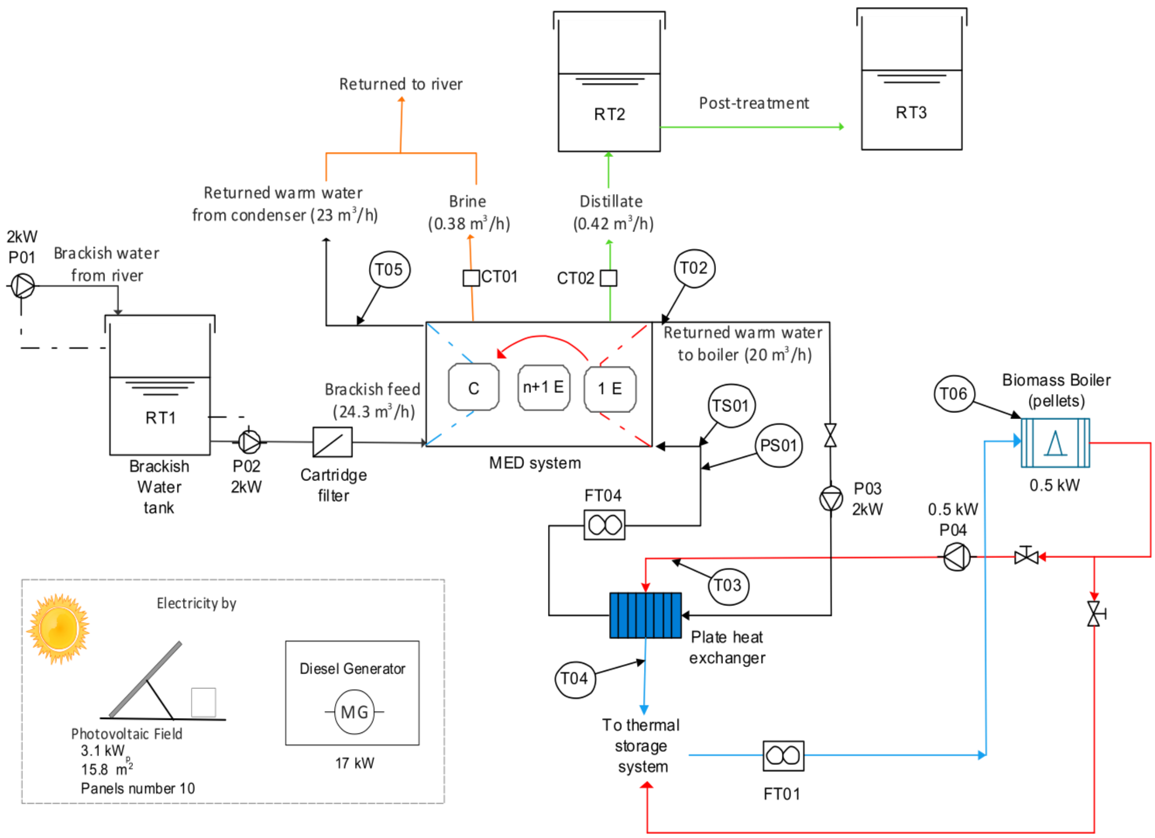

Fig. 2. General scheme of system

3. Techno-economic assessment

3.1 MED's effluents characterization

The characteristics of the brackish feed water from Camarones River and the effluents obtained from MED operation (brine and distillate) were gathered during several months. Average values are shown in Table 1 (the parameters of the waste stream returned to Camarones River were calculated by mass balance).

In order to determine the percentage of solutes remaining in the brine solution, the retention percentages are determined by Eq. 1. The results are shown in Table 1:

$$R(\%) = \frac{C_{BFW} - C_D}{C_{BFW}} \cdot 100 \qquad (1)$$

where C_{BFW} is the concentration of the corresponding parameter (As, B, Cd, Cu, etc.) in the brackish feed (mg/L) water and C_D the same one in the distillate water (mg/L).

Notice that all the retention percentages obtained were higher than 90% and more specifically B and As, that were removed in 95% and 99% respectively. As explained above, these are especially toxic elements for plants and humans, respectively.

Table 1
Characterization of brackish feed water, brine, distillate and waste stream

	Units	Brackish feed water	Brine	Distillate	R (%)	Waste stream (refrigeration + brine)
Flow	m^3/h	0.80	0.38	0.42	--	23.38
Total Disolved Solids (TDS)	mg/L	1,900	3,980	19.0	99	1,930
Conductivity	µS/cm	2,600	5,250	200	92	2,640
Arsenic (As_{total})	mg/L	0.60	1.26	0.006	99	0.61
Boron (B_{total})	mg/L	15.0	30.8	0.75	95	15.2
Cadmium (Cd^{+2})	mg/L	0.05	0.10	0.004	92	0.051
Calcium (Ca^{+2})	mg/L	210	430	8.4	96	213
Chlorides (Cl^{-})	mg/L	700	1,420	49.0	93	711
Copper (Cu^{+2})	mg/L	0.05	0.10	0.001	99	0.051
Iron (Fe_{total})	mg/L	0.20	0.40	0.016	92	0.20
Magnesium (Mg^{2+})	mg/L	25.0	52.0	0.25	99	25.4
Manganese (Mn^{+2})	mg/L	0.13	0.27	0.003	98	0.13
Plumb (Pb^{+2})	mg/L	0.03	0.06	0.003	91	0.030
Potassium (K^{+})	mg/L	35.0	72.0	1.8	95	35.6
Selenium (Se_{total})	mg/L	0.20	0.41	0.01	95	0.20
Sodium (Na^{+})	mg/L	200	420	2.0	99	203
Sulphates (SO_4^{2-})	mg/L	310	625	24.8	92	315
Zinc (Zn^{+2})	mg/L	0.30	0.62	0.006	98	0.31

3.2. Modelling and scale up of the solar water treatment system

3.2.1 MED plant

Taking the MED pilot plant located at the Taltape community as reference (8 stages, 10 m^3/day), a scale-up has been carried out for higher capacities, from 10 m^3/day to 5,000 m^3/day, in order to perform the economical assessment later. For this purpose, a design model of a MED plant with the same configuration as the one implemented in Taltape has been developed and implemented in Matlab. The MED model is based in the one published in (Palenzuela et al., 2014) but particularized for this study. In this model, unlike that the one described in our previous work, equal area in all effects was considered. For the computation of the model, an iteration loop was implemented in the Matlab software that starts with the temperature profile and continues until a convergence criterion is achieved. The convergence criterion of the model should have a maximum difference in effect areas of $1 \cdot 10^{-4}$ in order to achieve a good accuracy.

Firstly, the temperature difference between effects is obtained by the following equation:

$$\Delta T_{eff,i} = \frac{T_{v,1} - T_{v,N}}{N - 1} \tag{2}$$

where $\boldsymbol{N}$ is the number of stages, $\boldsymbol{T_{v,1}}$ is the vapor temperature generated in the 1_{st} effect and $\boldsymbol{T_{v,N}}$ is the vapor temperature generated in the last effect. In all cases, $\boldsymbol{N}$ has been established as 8 stages, $\boldsymbol{T_{v,1}}$ as 70 ºC and $\boldsymbol{T_{v,N}}$ as 35 ºC.

On the other hand, the area of each evaporator ($\boldsymbol{A_{ei}}$) is defined by the heat transfer equation. For the sake of simplicity, all the equations shown correspond to the first effect but can be extrapolated to the rest of effects:

$$Q_s = A_{e1} U_{e1} (T_s - T_{v1}) = M_s \lambda_s \tag{3}$$

where $\boldsymbol{Q_s}$ is the heat transfer rate provided to the first effect, $\boldsymbol{T_s}$ the temperature of the heating energy source supplied to the first effect of the MED plant, $\boldsymbol{T_{v1}}$ is the temperature of the vapor generated inside the first effect, $\boldsymbol{M_s}$ is the steam mass flow rate supplied as the heating energy source to the first effect, $\boldsymbol{\lambda_s}$ is the change in enthalpy related to the condensation of the steam supplied to the first effect, and $\boldsymbol{U_{e1}}$ is the overall heat transfer coefficient of the first evaporator. Notice that, although the heat transfer source provided to the first effect in the MED pilot plant of Taltape is hot water, for the high scale MED plants, steam has been considered as the energy source to match the commercial plants worldwide.

The overall heat transfer coefficient is determined by the correlation proposed by El-Dessouky and Ettouney (2002):

$$U_{e1} = 1.9695 + 1.2057 \cdot 10^{-2} T_{v1} - 8.5989 \cdot 10^{-5} T_{v1}^2 + 2.5651 \cdot 10^{-7} T_{v1}^3 \quad (4)$$

The ratio between the sum of all the evaporator areas to the distillate production is called specific area (**sA**) and it is a characteristic parameter that gives an idea of the size of the MED plants.

The mass flow rates of distillate and brine together with the temperatures of all the streams are determined by mass and energy balances in all the effects:

$$M_f = M_{gb,1} + M_{b,1} \quad (5)$$

where $\boldsymbol{M_{gb,1}}$ is the total vapor generated that, in turn, is converted to distillate when it condenses in the following effect, $\boldsymbol{M_f}$ is the feedwater mass flow rate and $\boldsymbol{M_{b,1}}$ is the brine flow rate that remain from the evaporation taking place in the first effect.

$$M_{gb,1}\lambda_{gb,1} = M_s\lambda_s - M_f C_p (T_{v1} - T_f) \quad (6)$$

where $\boldsymbol{\lambda_{gb,1}}$ the latent heat of vaporization at $\boldsymbol{T_{v1}}$, $\boldsymbol{C_p}$ is the specific heat and $\boldsymbol{T_f}$ the temperature of the feedwater that reaches the first effect of the MED plant.

One of the parameters that evaluates the performance of the MED plant is the Recovery Ratio (**RR**), which is defined as the ratio of the total distillate obtained from the plant ($\boldsymbol{M_{prod}}$) to the feed water flow rate ($\boldsymbol{M_f}$):

$$RR = \frac{M_{prod}}{M_f} \quad (7)$$

This parameter has been established as an input in the model of the MED plant and a value of 50% has been considered in all cases (this is a fair value when low salinity feed water is being treated by an MED plant).

Another performance parameter is the specific thermal consumption ($\boldsymbol{STC}$), which is defined as the thermal energy supplied to the plant ($\boldsymbol{Q_s}$) for the total distillate obtained from the plant:

$$STC = \frac{Q_s}{M_{prod}} \quad (8)$$

The third performance parameter of this kind of plants is the Gain Output Ratio ($\boldsymbol{GOR}$) which is defined as the mass flow rate of distillate produced per consumed heating steam rate:

$$GOR = \frac{M_{prod}}{M_s} \quad (9)$$

3.2.2. Thermal solar field

The thermal solar field has been sized for all the sizes of the MED plant (from 10 m^3/day to 5,000 m^3/day) and the results in terms of total aperture area have been used in the economic assessment. It has been considered as a solar field composed by evacuated tube collectors (ETC) to supply the thermal energy required by the MED plant, since they are the ones with the highest efficiency among the static solar collectors. The selected collector is from the company sunflower renewable energy Co. (model SF-BF305818) whose technical characteristics are shown in Table 2.

Table 2
Characteristics of the ETC (results of EN 12975 test results)

Aperture area: 2.83 m^2

Longitudinal incidence angle modifier	θ_L=10º: 1.00
	θ_L=20º: 1.00
	θ_L=30º: 0.99
	θ_L=40º: 0.97
	θ_L=50º: 0.92
	θ_L=60º: 0.84
	θ_L=70º: 0.68
Tangential incidence angle modifier	θ_T=10º: 1.04
	θ_T=20º: 1.09
	θ_T=30º: 1.23
	θ_T=40º: 1.38
	θ_T=50º: 1.78
	θ_T=60º: 1.82
	θ_T=70º: 2.08
Efficiency parameters	η_{opt}: 0.64
	c_1: 1.494 W/ K·m^2
	c_2: 0.012 W/ K^2·m^2
Flow rate: 0.020 kg/s·m^2	

η_{opt}, c_1 and c_2 are the optical efficiency and the coefficients accounting for thermal losses, respectively.

The collectors are orientated to the North and with a tilt angle equal to the local latitude. The location of Taltape has the following geographical coordinates: lat. 18.99° S, long. 69.77° W. For the size of the solar field, a design point (specific date, including month, day and time) is firstly selected from a typical meteorological year (TMY) that has been obtained with Meteonorm software for the specific location. The design point selected has been 19th of June at solar noon (this time corresponds to sun zenith and presents greater stability of the direct solar irradiation) due to the good weather conditions, which can lead to higher solar operation hours of the water treatment plant. Also, a solar multiple of 2 has been considered in order to have an annual solar contribution close to 50% (it means higher hours of solar operation for the water treatment system).

Table 3 shows the monthly data of global irradiation over tilted plane (G_k) and ambient temperature (T_{amb}).

Table 3
Data of irradiation and ambient temperature of a TMY in Taltape, Arica

Month	G_k [kWh/m^2]	T_{amb} [ºC]
January	190	19.9
February	173	20.2
March	188	19.4
April	154	16.9
May	136	14.2
June	110	12.4

July	119	11.9
August	137	11.9
September	154	12.6
October	180	14.3
November	186	16.1
December	186	18.2

The global irradiation data has been normalized with the actual measurement of the yearly global irradiation over a tilted plane (G_k, 2,110 kWh/m^2·y) obtained from a radiometric measuring solar station located close to the selected location.

The design of the solar field is carried out by firstly determining the number of collectors in series in a row and secondly the number of rows in parallel.

On one hand, the number of collectors in series in a row is determined by the ratio between the temperature increase required in a row and the temperature step of an individual solar collector. The outlet temperature reached at the outlet of the collector is determined by the efficiency equation of the collector:

$$\eta_i = \frac{\dot{m}C_p(T_{out} - T_{in})}{G_k A_a} = \eta_{opt}K_{\tau\alpha} - c_1\left[\frac{(T_{col} - T_{amb})}{G_k}\right] - c_2\left[\frac{(T_{col} - T_{amb})^2}{G_k}\right] \tag{10}$$

where $\dot{\boldsymbol{m}}$ is the heat transfer fluid (i.e. water) mass flow rate through the solar collector; $\boldsymbol{C_p}$ is the average heat capacity of the heat transfer fluid; $\boldsymbol{T_{col}}$ is the average between the inlet and outlet temperatures of the collector; $\boldsymbol{T_{in}}$ and $\boldsymbol{T_{out}}$ are the inlet and outlet temperatures in the solar collector, respectively; $\boldsymbol{G_k}$ is the global solar irradiance on tilted plane in W/m^2, $\boldsymbol{A_a}$ is the aperture area of the collector and $\boldsymbol{K_{\tau\alpha}}$ is the incident angle modifier, which is determined as the product between the longitudinal and tangential incident angle modifiers (see Table 2):

$$K_{\tau\alpha} = K_{\tau\alpha}(T) \cdot K_{\tau\alpha}(L) \tag{11}$$

Considering the operational temperature of the MED plant between 65 ºC and 75 ºC, a temperature increase in the solar field from 75 ºC to 85 ºC has been established for the calculation.

On the other hand, the number of rows is determined as the ratio between the thermal power to be supplied by the solar field (that is the thermal power required by the MED plant, which is defined by the specific thermal consumption and distillate production of the plant) and the thermal power supplied by one individual row. This last one is determined from the thermal power supplied by one collector (according to equation 10), multiplied by the number of collectors connected in series. The product of the number of collectors connected in series and the number of rows gives the total number of collectors required by the solar field that multiplied by the aperture area of one collector, leads to the total area of the solar field.

Finally, an annual simulation model of the dimensioned solar field developed by the authors (Andrés-Mañas et al., 2017) has been used to determine the hours of operation of the water treatment plant with solar energy for all MED plant capacities. The model determines the thermal power supplied by the solar field every hour by an iteration loop that recalculates the flow rate through the solar field as a function of the outlet temperature reached. The hours of solar operation are considered when the hourly power provided by the solar field is higher than the 50% of the MED thermal load. The model also gives the solar fraction, which is defined as the relation between the amount of energy obtained through the solar technology used and the total annual energy required by the process. The amount of energy obtained through the solar technology is determined as the sum of the thermal power provided in each interval multiplied by the time interval, and the total energy required by the process as the thermal power multiplied by the hours of operation and by the total days in the year. Also, the model gives the annual fresh water produced by the MED plant with the thermal energy provided by the solar field. The definition of Gain Output Ratio has been used for this purpose.

3.3 Economical assessment

The economical assessment was done using the data obtained from the plant installed at Taltape (10 m^3/day), which includes actual data about the system implementation and operation. The plant scaling up was carried out up to 5000 m^3/day, which is considered the water production needed to supply the nearest city located at the same Chilean region as Taltape, named Arica, with approximately 200,000 inhabitants. For the evaluation of the scaling up effect, 10, 200, 500, 1,000, 2,500 and 5,000 m^3/day have been taken as the production capacities. In addition, 350 operating days per year were taken into account, corresponding to a water production of $3.5 \cdot 10^3$ m^3/yr for the smallest MED plant and $1.75 \cdot 10^6$ m^3/yr for the biggest MED plant considering a 24/7 operating regime. According to (Papapetrou et al., 2017), it is necessary to define boundary conditions for the cost calculation. In this work, post-treatment of distilled water is excluded as well as water distribution, laboratory for quality control and distillation plant decommissioning at the end-of-life. Chemical costs included in the calculation were (industrial-grade prices obtained from Chilean companies): pellets for biomass boiler 0.17 USD$/kg -price provided by PROENERGY S.L. (VIII region, Chile); Diesel for generator 0.63 USD$/L -price provided by PETRONOR S.L. (XV region Chile); Oil and refrigerant for maintaining of generator motor was 7.2 and 7.4 USD$/L, respectively -prices provided by SODIMAC S.L. (XV region, Chile); anti-fouling model GMP 670 was 8.7 USD$/L -prices provided by GENESYS MEMBRAM PRODUCTS (Metropolitan region, Chile)-.

For the scaling of the main equipment, the costs can be obtained by the Rule of Six Tenths (Seider et al. 2004) if the cost of a similar item of different size or capacity is known. The following equation, Eq. 12, expresses the rule of six-tenths:

$$C_B = C_A \cdot \left(\frac{S_B}{S_A}\right)^n \tag{12}$$

where C_B represents the approximate cost (USD$) of equipment having size S_B (kW, Hp, m^2, or whatever). C_A is the known cost (USD$) of equipment having a corresponding size S_A (same units as S_B), and $\frac{S_B}{S_A}$ is the ratio known as the size factor, dimensionless. The size factor's exponent, "n", depends on the equipment type and it can vary from 0.3 to 1 with an average value near 0.6 (see Table 4) (Couper, 2002).

Table 4

Size factor, interest and period of amortization

Main equipment	Size factor's exponent (n)	Interest rate (i, %)	Depreciation period (t, years)
MED	0.53	5	20
Biomass boiler	0.50	5	10
Diesel generator	0.60	5	5
Solar fields (thermal and PV)	0.60	5	15

The water treatment costs are calculated by the Simplified Cost of Water (SCOW) method (Papapetrou et al., 2017) using Eq.13.

$$SCOW = \frac{C_F + C_v}{M_w} \tag{13}$$

where M_w is the annual volume of water produced, C_F the annual fixed costs and C_v operating costs.

The annual fixed costs (Eq. 14) include the construction of the plant (amortization of the equipment and material), engineering, construction and project management, initial design and permitting and land cost (Papapetrou et al., 2017). According to (Papapetrou et al., 2017), normally, most of these costs are ignored and these are presented as an approximated percentage of the main equipment costs. In this case, the initial design, engineering, construction and project management costs were considered to be included in the MED plant facility cost as it was provided by INERCO Tratamiento de Aguas S.A. In addition, the Municipality of Camarones handed over the land and gave the corresponding permissions free of charge. Normally, the cost of land is never considered as it greatly depends on the plant geographical location.

$$C_F = \sum I_o \cdot \alpha \tag{14}$$

$$\alpha = \left(\frac{i}{1-(1+i)^{-t}}\right) \tag{15}$$

where I_o is the initial capital investment, α the amortization factor, i is discount rate and t is depreciation period in years.

On the other hand, the variable costs (or operating costs) (Eq. 16) include: reagents and chemical consumptions ($C_{consumables}$), energy needed, staff (C_{staff}) and maintenance of the facility ($C_{maintenance}$). Regarding the energy needed, electricity consumption was not considered as operating cost because there is no electric network available in the Taltape community (as already mentioned, a diesel generator is used to supply the electric energy when solar radiation is not available). In this way, the diesel and pellet consumptions used to generate on-site energy are considered within the operating costs ($C_{consumables}$), while the diesel generator and boiler were considered as main equipment in the annual fixed costs.

$$C_v = \left(C_{consumables} + C_{staff} + C_{maintenance} \right) \tag{16}$$

4. Results and discussion

4.1. Dimensioning of the MED and solar thermal field

Table 5 shows the results obtained from the design of the MED plant for distillate productions of 200, 500, 1,000, 2,500 and 5,000 m^3/day. As shown in the Table 5, the GOR obtained was 6.9 considering MED plants of 8 stages and a temperature lift (temperature difference between the vapor temperature inside the first and last effects) of 35 ºC. As expected, the thermal power required by the distillation process increases proportionally with the plant capacity. These values were used to scale up the kW_{th} needed in the biomass boiler and the kW_e needed in the diesel generator.

Table 5
Results from the design of the MED plant with different distillate production. All the variables are described in the nomenclature

	200 m^3/day	500 m^3/day	1,000 m^3/day	2,500 m^3/day	5,000 m^3/day
Q_s (kW_{th})	775	1937.5	3,875	9,687.5	19,375
M_s (kg/s)	0.4	0.8	2.0	3.3	8.0
GOR	6.9	6.9	6.9	6.9	6.9
M_f (m^3/h)	18	38	100	165	400

A_{ef} (m^2)	74	170	427	705	1,708
P_e (kW_e)*	18.3	45.8	91.7	229.2	458.3

*P_e is the total electric power consumed by the MED plant, which has been determined assuming a specific electric consumption of 2.2 kWh/m^3 for all cases.

Regarding the solar thermal field, Table 6 shows the results corresponding to the pilot plant installed in Taltape. The resulting solar thermal field is formed by 40 ETC with a total aperture area of 113.2 m^2 and an outlet temperature from a solar collector of 88.1 ºC.

Table 6
Solar thermal field dimensioning results for the pilot MED plant located in Taltape

Variables	Values
T_{out}	88.1 ºC
N_{col_series}	1
N_{rows}	40
N_{total}	40
A_T	113.2 m^2

In order to have a better representation of the behavior of the MED pilot plant located at Taltape with the solar field and biomass boiler, monthly simulations have been performed to determine the solar fraction (F_s) and the fresh water produced every month. The results are represented in Fig. 3. The highest solar fraction was obtained in March, 57.8%, which nearly doubled the solar fraction of the worst month, June, with 31.6%. The annual average solar fraction was 46.6%, which is represented in Fig. 3 as a dotted line, and the annual energy provided by the solar field was 560.9 GJ.

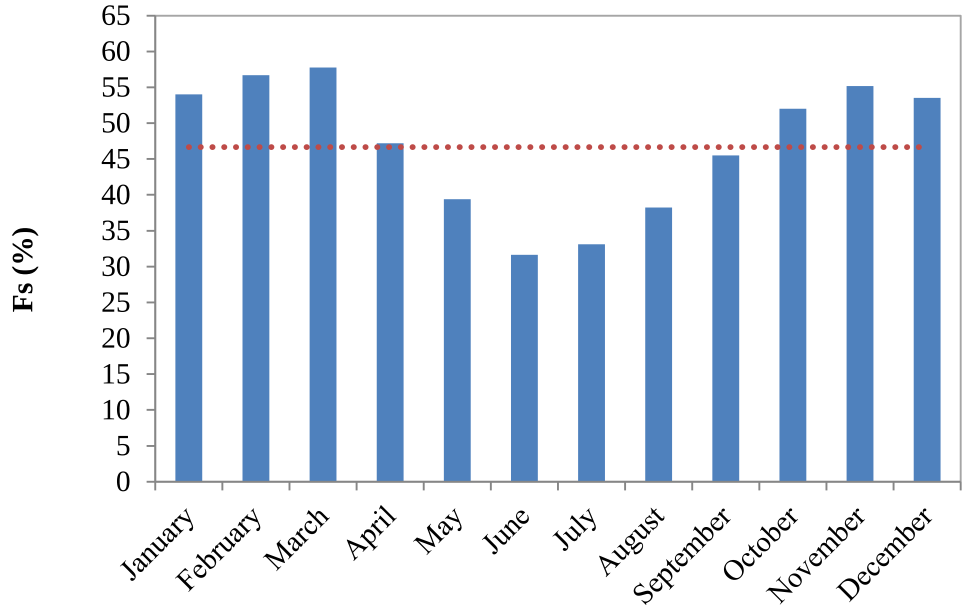

Fig. 3. Monthly solar fraction in Taltape, Arica (blue bars) and annual average solar fraction (red dotted line).

The ratio between the monthly fresh water produced by solar energy and the monthly fresh water demanded and the same ratio but with the monthly fresh water produced by the biomass boiler (red bars) has been determined in order to have an idea of the solar operation of the MED plant (see Fig. 4). The fresh water demanded is the amount of drinking water, domestic and hygiene use established by UNESCO. As expected, the MED plant will operate mostly with solar energy during summer and spring months (January, February, March, October, November and December), covering between 85-95% of the freshwater only with solar energy. During autumn and winter months (from April to September), the percentage of use of the boiler is higher, reaching a percentage of nearly 50% in June. From the annual simulation, a total fresh water production with the MED operating with the thermal energy provided by the solar field of 1,690 m^3 was obtained, which means a total of 2,823 hours of solar operation.

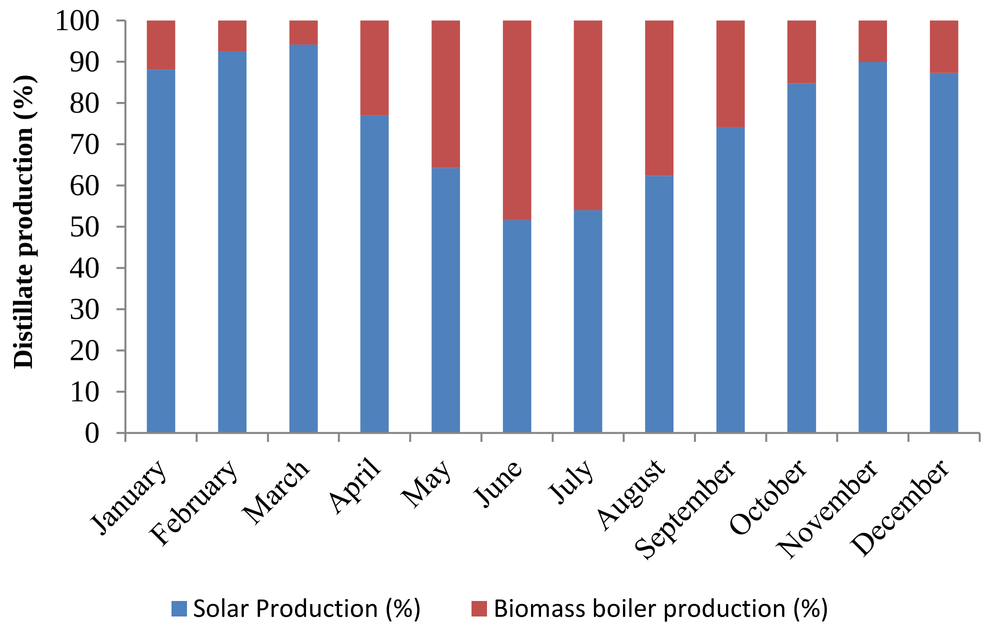

Fig. 4. Relative fresh water production with respect the water demand established by UNESCO, using solar thermal energy (blue bars) and using the biomass boiler (red bars) along the year.

For the rest of cases (the scales-up to higher fresh water capacities), Table 7 shows the size of the solar thermal field in terms of total number of collectors (N_T) and total aperture area (A_T), the annual thermal energy provided by the solar field (E_{SF}), the annual fresh water produced by solar energy (F_{SW}) and the annual hours of solar operation (H_{op}) of the MED plant. As can be seen, the solar fraction and hours of operation are kept almost constant in all cases. The rest of parameters are increased in the same scale factor as the capacity (2.5).

Table 7
Results from the dimensioning of the solar thermal field and from the annual simulation of the solar water treatment system

MED capacities (m^3/day)	N_T	A_T	F_s (%)	E_{SF} (GJ)	F_{SW} (m^3)	H_{op} (h)
200	838	2372	48.9	$1.2 \cdot 10^4$	$3.5 \cdot 10^4$	2861
500	2100	5943	49.0	$3.0 \cdot 10^4$	$8.9 \cdot 10^4$	2863

1000	4202	11892	49.0	$6.0\cdot10^4$	$1.8\cdot10^5$	2864
2500	10504	29726	49.0	$1.5\cdot10^5$	$4.4\cdot10^5$	2864
5000	21006	59447	49.0	$3.0\cdot10^5$	$8.9\cdot10^5$	2864

4.2. Economical assessment

The initial capital costs (I_0 in USD$) accounting for the MED plant, which correspond to the biomass boiler, the diesel generator (installed elements) and the solar thermal and photovoltaic fields are shown in Table 8, together with the annual fixed costs (C_F both in USD$ and USD$/m^3). These costs include the actual values paid to the supplier companies that participated in this initiative (INERCO Tratamiento de Aguas S.A. Madrid, Spain –MED plant-, VIELCO Company –diesel generator- and Nueva Energía –boiler- and SOLUTECHNO, Perú –solar photovoltaic fields-) and a quotation provided by SOLUTECHNO, Perú, according to the results obtained from the size of the solar thermal field. Then, the investment costs for the 10 m^3/day size plant are: 579 USD$/m^2 for the solar thermal installation including storage, 8.0 USD$/W$_p$, 9,400 USD$ for the diesel generator and 11,600 USD$ for biomass boiler and an initial capital cost of 139,900 USD$ for the water treatment unit (MED). Assuming the amortization periods and interest rates shown in Table 4, the annual fixed cost for the main equipment of the system can be calculated. Notice that only the cost variation caused by the plant scaling up from 10 m^3/day to 200 m^3/day is analyzed in detail in this section in order to simplify the discussion (see Tables 8 and 9). Thus, Table 9 shows the breakdown of the operating costs for the MED plant installed (10 m^3/day) and scaled up (200 m^3/day). When calculating the SCOW, the results are shown in Table 10 for all water treatment capacities considered in this study (from 10 to 5,000 m^3/day).

Table 8
Initial capital costs (I_0) and annual fixed costs (C_F) for the main equipment

Treatment capacity		MED plant	Biomass boiler	Diesel generator	Solar thermal and PV fields	Total
10 m^3/day	I_0 (USD$)	139,900	11,600	9,400	90,500	251,400
	C_F (USD$)	11,200	1,500	2,200	8,700	23,600
	C_F/M_w (USD$/$m^3$)	3.2	0.4	0.6	2.5	6.7
	Relative cost (%)	47.5	6.1	8.9	35.4	-
200 m^3/day	I_0 (USD$)	684,500	51,900	30,000	561,500	1,327,900
	C_F (USD$)	54,900	6,700	4,850	54,100	120,550
	C_F/M_w (USD$/$m^3$)	0.78	0.10	0.07	0.77	1.7
	Relative cost (%)	45.5	5.3	3.9	43.2	
	Reduction (%)	75.6	75.0	88.3	69.2	74.6

It should be highlighted that the MED plant implementation together with the solar fields, represent the higher relative C_F of the main equipment, concretely 3.2 and 2.5 USD$ per m^3 treated at the smallest scale, respectively (see Table 8). If the treatment capacity of the MED plant is increased to 200 m^3/day, these costs can be reduced to 0.78 and 0.77 USD$ per m^3 treated, following the same order. Also, the C_F of the diesel generator and biomass boiler can be diminished considerably, 88.3 and 75.0% respectively. Thus, the total annual fixed costs per m^3 treated are reduced in 74.6%, i.e. from 6.7 USD$ per m^3 to 1.8 USD$ per m^3.

On the other hand, the breakdown of operating consumptions is summarized in Table 9. As commented in previous sections, the costs were obtained considering 350 operating days per year that correspond to $70 \cdot 10^3$ m^3 treated per year and 24/7 operating regime and were also scaled from 10 m^3/day to 200 m^3/day. The operating and maintenance costs were obtained taking into account the reagents and chemical consumptions shown in Section 3.3 The main consumptions are also described in Table 9. The maintenance cost was considered as 2% of annual fixed cost according (Papapetrou et al., 2017) and the staff costs were considered as 0.03 USD$ per m^3 treated (Kesieme et al., 2013). The chemicals and consumables taken into account were: (i) Anti-fouling with a consumption of 0.01 L/h for 10 m^3/day and 0.02 L/h for 200 m^3/day. The anti-fouling consumptions was provided by INERCO. This consumption is only considered in the inlet to to the process. (ii) Diesel consumptions was considered 3.7 L/h for 12 kW_e for 10 m^3/day and 5.9 L/h for 45.8 kW_e for 200 m^3/day. The data of diesel consumptions were obtained from Worldwide Power Products LLC, approximate the fuel consumptions of a diesel generator based on the size of the generator; (iii) Oil consumptions was considered that each 250 h of operation the oil must be changed 6.5L; (iv) Refrigerant consumptions was considered that each 1,000 h of operation the refrigerant must be changed 8L; (v) the biomass consumption were calculated as 4.9 kg/h for 38,6 kW_{th} for 10 m^3/h and 63.2 kg/h for 775 kW_{th} for 200 m^3/h, (vi) and finally the Sulfamic acid 5% was considered as acid cleaning once per year.

Table 9
Breakdown of operating costs for MED plant installed (10 m^3/day) and scaled up (200 m^3/day)

Operating costs	10 m^3/day			200 m^3/day		
	C_v	Relative cost	C_v/M_w	C_v	Relative cost	C_v/M_w
	USD$	%	USD$/$m^3$	USD$	%	USD$/$m^3$
Staff (0.03 USD$/$m^3$)[a]	110	0.4	0.03	2,100	1.8	0.03
Maintenance (2% I_0)[b]	5,100	18.2	1.46	26,400	22.4	0.39
Chemicals and consumables						
Anti-fouling (0.01 L/h)	950	3.4	0.27	1,900	1.6	0.03
Diesel consumptions Semi-industrial, 10 m^3/day: 12 kW_e consumption 3.7 L/h MED plant scaled, 200 m^3/day: 45.8 kW_e consumption 5.9 L/h	12,800	45.6	3.7	20,600	17.5	0.29
Oil (change each 250 h, 6.5L)	1,350	4.8	0.38	3,000	2.6	0.04
Refrigerant (change each 1000 h, 8L)	250	0.9	0.07	500	0.4	0.007
Biomass: Pellets	7,400	26.4	2.1	63,000	53.6	0.9

Semi-industrial, 10 m^3/day: 38,6 kW_{th} consumption 4.9 kg/h MED plant scaled, 200 m^3/day: 775 kW_{th} consumption 63.2 kg/h						
Sulfamic Acid 5% (once per year)	75	0.3	0.02	75	0.06	0.001
TOTAL	28,035		8.0	117,575		1.7

[a]Kesieme et al., 2013, [b]Papapetrou et al., 2017

The diesel and biomass consumptions together with the maintenance, represent the most important part of the operating costs associated with the treatment both at small (10 m^3/day) and large scale (200 m^3/day). Previously, the highest cost was the diesel consumption, 3.7 USD$/$m^3$, which represents 45.6% of the total operating costs, followed by the pellets consumption (2.1 USD$/$m^3$, 26.4 % relative cost) and maintenance (1.48 USD$/$m^3$, 18.2% relative cost). However, the order changes at large scale (from 200 to 5,000 m^3/day), where the pellets consumption presents by far the highest relative cost (0.9 USD$/$m^3$, 53.6%), followed by maintenance (0.39 USD$/$m^3$, 22.4%) and diesel consumption (0.29 USD$/$m^3$, 17.5%). The absolute increase in the diesel consumption due to the scaling up of the solar water treatment system is much lower than the absolute increase in the pellets consumption. Antifouling chemicals and oil for the electric generator represent about a 4% relative cost each at small-scale and about 2% each at large-scale while staff salaries and sulfamic acid consumption present almost negligible costs regardless of the scale. The solar water treatment system scaling up allows a reduction of 78.7% in the total operating costs, which diminished from 8.0 USD$ per m^3 treated for small scale to 1.7 USD$ per m^3 treated for large scale.

The cost of distillated water produced by the MED plant, SCOW, varies from 15.0 USD$/$m^3$ for the 10 m^3/day production capacity to 3.2 USD$/$m^3$ when this variable is increased to 200 m^3/day, which is equivalent to a 76.7% reduction (see Table 10). These high costs obtained are clearly affected by the economy of scale and, mainly, due to use of diesel generator and biomass boiler, since the water treatment system is located in a remote arid area where the lack of electric grid and transport is a determinant factor.

As has been expressed during the whole study, the plant treatment capacity is extremely important for the SCOW. Therefore, a final study in which the relationship between these two variables is analyzed was carried out and it is presented in Fig. 5 and Table 10. These costs were calculated following the same sequence explained in Section 3.3. The highest cost reduction was observed in the case exposed above, i.e. when the MED production capacity was increased from 10 to 200 m^3 per day, resulting in 76.7% SCOW reduction. The next analyzed level was 500 m^3/day, which represented 37.1% SCOW improvement with respect to the previous case while varying from 500 m^3/day to 1,000 m^3/day resulted in 20.2% SCOW decrease. Thus, increasing the MED treatment capacity always results in the improvement of the SCOW. However, this improvement gets lower with each MED treatment capacity increase so that, finally, it becomes negligible.

Table 10

The SCOW and reduction percentage achieved for different treatment capacities.

Treatment capacity (m^3/day)	SCOW (USD$/$m^3$)	Reduction percentage (%)
10	15.0	
200	3.20	76.7
500	2.20	85.3
1,000	1.76	88.3
2,500	1.40	90.7
5,000	1.25	91.6

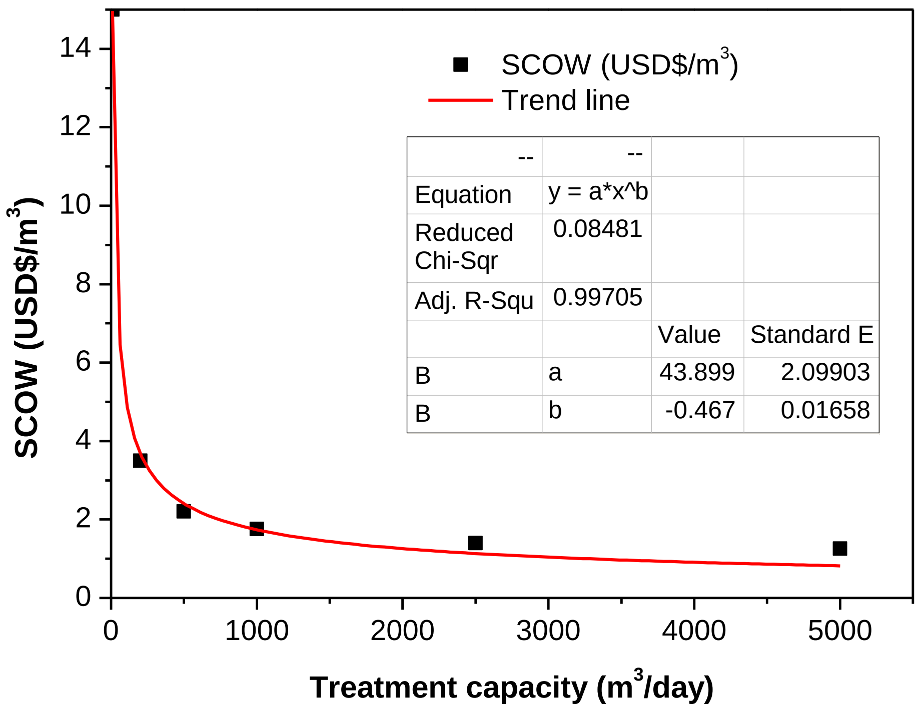

Fig. 5. Simplified Cost of Water (SCOW) versus treatment capacity (m^3/day).

4. Conclusions

This paper presents the simulation of a MED pilot plant located in a remote community of the north of Chile (Taltape) that will be used to improve its agricultural activity and for domestic and hygiene purposes. From the operation of this plant, it has been demonstrated that the water treatment process allows diminishing As and B in 99% and 95%, respectively. The water treatment system will be coupled to a static solar thermal field to make it more sustainable taking advantage of the high solar radiation of the location. The whole system has been simulated along a whole year using meteorological data from Taltape in order to assess the solar operation of the water treatment plant and determine the use of a biomass boiler as a backup when the solar radiation is not available. An annual solar fraction of 46.6% and a total fresh water production with the MED operating with solar energy of 1,690 m^3 have been obtained, which make a total of 2,823 hours of exclusive solar operation. It means that the needs of the community can be fully covered during most of the year with the solar field, making a higher use of the biomass boiler (up to 48%) from May to August.

An economic assessment has been also performed in order to study the water costs of the MED pilot plant and they scaled up to 5,000 m^3/day. The cost of distillated water produced by the MED plant varied from 15.0 USD$/$m^3$ for the 10 m^3/day production capacity to 1.25 USD$/$m^3$ when this variable is increased to 5,000 m^3/day, which is equivalent to a 91.6% reduction. It was found that the MED plant implementation and solar fields represent the higher relative annual fixed cost of the main equipment while the diesel and biomass consumptions together with the maintenance represent the most important part of the operating costs.

Acknowledgments

PhD. Lorena Cornejo Ponce wishes to thank the Region Government of Arica&Parincota (FIC Taltape BIP code 30158422-0). PhD. Sara Miralles-Cuevas wishes to thank the Solar Energy Research Center for her post-doctoral position in Arica, Chile, under SERC-Chile, FONDAP project (reference: 15110019). PhD. Alejandro Cabrera wishes to thank his post-doctoral position at University of Tarapacá. Patricia Palenzuela wishes to thank funding support from the Spanish Ministry of Economy and Competitiveness and ERDF funds under the National R+D+I Plan Project DPI2014-56364-C2-2-R.

References

Abejón, A., Garea, A., Irabien, A., 2015. Arsenic removal from drinking water by reverse osmosis: Minimization of costs and energy consumption, Separation and Purification Technology 144, 46-53.

Andrés-Mañas, J.A., Palenzuela, P., Cornejo, L., Alarcón-Padilla, D.C., Acién, G., Zaragoza, G., 2017. Preliminary evaluation of the use of vacuum membrane distillation for the production of drinking water in Arica (Chile), Desalination & Water Treatment 61, 160-169.

Bhattacharjeea, P., Chatterjeea, D., Singhb, K., Giri, A., 2013. Systems biology approaches to evaluate arsenic toxicity and carcinogenicity: an overview. Int. J. Hyg. Environ. Health. 216, 574–586.

Bick, A., Oron, G., 2005. Post-treatment design of seawater reverse osmosis plants: Boron removal technology selection for potable water production and environmental control, Desalination 178, 233–246.

Bundschuh, J., Litter, M., Ciminelli, V.S.T., Morgada, M.E., Cornejo, L., Hoyos, S.G., Hoinkis, J., Alarcón-Herrera, M.T., Armienta, M.A., Bhattacharya, P., 2010. Emerging mitigation needs and sustainable options for solving the arsenic problems of rural and isolated urban areas in Latin America - A critical analysis. Water Research 44 (19), 5828-5845.

Choong, T.S.Y., Chuah, T.G., Robiah, Y., Gregory Koay, F.L., Azni, I., 2007. Arsenic toxicity, health hazards and removal techniques from water: an overview, Desalination 217 (1-3), 139-166.

Chorak, A., Palenzuela, P., Alarcón-Padilla, D.C., Abdellah, A.B., 2017. Experimental characterization of a multi-effect distillation system coupled to a flat plate solar collector field: empirical correlations, Applied Thermal Engineering 120, 298-313.

Couper, J.R., 2002. Process Engineering Economics, Chapter 4, page 70, CRC Press Ed.

Darwish, M., Hassan, A., Mohtar, R., 2013. Toward Implementing HH the Amir Declaration of 2% Electricity Generation by Solar Energy in 2020, Energy and Power Engineering 5, 245-258.

Decreto Supremo 143/2009. Normas de calidad primaria para las aguas continentales superficiales aptas para actividades de recreación con contacto directo (https://www.leychile.cl/Navegar?idNorma=288386).

Decreto Supremo 144/2009. Normas de calidad primaria para la protección de las aguas marinas y estuarinas aptas para actividades de recreación con contacto directo (https://www.leychile.cl/Navegar?idNorma=1001042).

Directive 98/83/EC. European Union, Council Directive 98/83/EC on the quality of water intended for human consumption.

El-Dessouky, H., Ettouney, H., 2002. Fundamentals of Salt Water Desalination, 1ª ed. Amsterdam, The Netherlands: ELSEVIER SCIENCE B.V, 2002.

El-Nashar, A.M. and Ishii, K., 1985. Abu Dhabi solar distillation plant, Desalination 52, 217-234.

El-Nashar, A.M., Qamhiyeh, A.A., 1995. Simulation of the steady-state operation of a multi-effect stach seawater distillation plant, Desalination 101, 231-243.

Fernández-Izquierdo, P., García-Rodríguez, L., Alarcón-Padilla, D., Palenzuela, P., Martín-Mateos, I., 2012. Experimental analysis of a multi-effect distillation unit operated out of nominal conditions, Desalination 284, 233-237.

GLASS Report, 2014. UN-Water Global Analysis and Assessment of Sanitation and Drinking-Water GLAAS Report.

Hanel, M., Escobar, R., 2013. Influence of solar energy resource assessment uncertainty in the levelized electricity cost of concentrated solar power plants in Chile, Renewable Energy 49, 96-100.

Hilal, N., Kim, G.J., Somerfield, C., 2011. Boron removal from saline water: A comprehensive review, Desalination 273, 23–35.

Hong-Jie, S., Bala, R., Bing, W., Jun, L., Li-Ping, P., Lena, M., 2014. Arsenic and selenium toxicity and their interactive effects in humans. Environ. Int. 69, 148–158.

Kesieme, U.K., Milne, N., Aral, H., Cheng, C.Y., Duke, M., 2013. Economic analysis of desalination technologies in the context of carbon pricing, and opportunities for membrane distillation, Desalination 323, 66–74, http://dx.doi.org/10. 1016/j.desal.2013.03.033.

Li, C., Goswami, Y., Stefanakos, E., 2013. Solar assisted sea water desalination: a review, Renew. Sust. Energ. Rev. 19, 136-163.

López, D.L., Bundschuh, J., Birkle, P., Armienta, M.A., Cumbal, L., Sracek, O., Cornejo, L. , Ormachea, M., 2012. Arsenic in volcanic geothermal fluids of Latin America, Science of the Total Environment 429, 57–75.

Mohtar, R. and Darwish, M., 2013. Prime Energy Challenges for Operating Power Plant in GCC, Energy and Power Engineering 5, 109-128.

Öztürk, N., Kavak, D., Köse, T.E., 2008. Boron removal from aqueous solution by reverse osmosis, Desalination 223, 1–9.

Palenzuela, P., Hassan, A.S., Zaragoza, G., Alarcón-Padilla, D.C., 2014. Steady-state model for multi-effect distillation case study: Plataforma Solar de Almería MED pilot plant, Desalination 337, 31-42.

Palenzuela, P., Alarcón-Padilla, D.C., Zaragoza, G., 2016. Experimental parametric analysis of a solar pilot-scale multi-effect distillation plant, Desalination & Water Treatment 57, 23097-23109.

Papapetrou, M., Cipollina, A., La Commare, U., Micale, G., Zaragoza, G., Kosmadakis, G., 2017. Assessment of methodologies and data used to calculate desalination costs, Desalination 419, 8-19.

Seider W.D., Seader J.D., Lewin D.R., 2004. Product and Process Design Principles: Synthesis, Analysis and Evaluation, 2nd Ed, Wiley.

Valenzuela, C., Mata-Torres, C., Cardemil, J.M., Escobar, R.A., 2017. CSP+PV hybrid solar plants for power and water cogeneration in northern Chile, Solar Energy 157, 713-726.

Wang, Q., Zhang, G.S., Chen, H., Wang, P., 2016. Enhanced As(III) removal at low concentrations by the combined pre-oxidation and nanofiltration membrane process, Desalination and Water Treatment 57 (59), 28947-28956.

WHO, 2016. Evaluations of the Joint FAO/WHO Expert Committee on Food Additives (JECFA): arsenic data. http://www.who.int/mediacentre/factsheets/fs372/en/

WHO and UNICEF, 2017. Progress on drinking water, sanitation and hygiene: 2017 update and SDG baselines. Geneva: World Health Organization (WHO) and the United Nations Children’s Fund (UNICEF), 2017. Licence: CC BY-NC-SA 3.0 IGO. ISBN 978-92-4-151289-3.

Yang, Y., Lior, N., 2006. Performance analysis of combined humidified gas turbine power generation and multi-effect thermal vapour compression desalination systems Part1: the desalination unit and its combination with a steam-injected gas turbine power system, Desalination 196, 84–104.

Yunus, M., Sohel, N., Kumar Hore, S., Rahman, M., 2011. Arsenic exposure and adverse health effects: a review of recent findings from arsenic and health studies in Matlab, Bangladesh. Kaohsiung. J. Med. Sci. 27, 371–376.